Inorganic Chemistry

Article

pubs.acs.org/IC

New Structure Type in the Mixed-Valent Compound $YbCu_4Ga_8$

Udumula Subbarao,[†] Matthias J. Gutmann,[‡] and Sebastian C. Peter*,[†]

[†]New Chemistry Unit, Jawaharlal Nehru Centre for Advanced Scientific Research, Jakkur, Bangalore, 560064, India

[‡]ISIS Facility, STFC-Rutherford Appleton Laboratory, Didcot, OX11 OQX, United Kingdom

Supporting Information

ABSTRACT: The new compound $YbCu_4Ga_8$ was obtained as large single crystals in high yield from reactions run in liquid gallium. Preliminary investigations suggest that $YbCu_4Ga_8$ crystallizes in the $CeMn_4Al_8$ structure type, tetragonal space group $I4/mmm$, and lattice constants are $a = b = 8.6529(4)$ Å and $c = 5.3976(11)$ Å. However, a detailed single-crystal XRD revealed a tripling of the c axis and crystallizing in a new structure type with lattice constants of $a = b = 8.6529(4)$ Å and $c = 15.465(1)$ Å. The structural model was further confirmed by neutron diffraction measurements on high-quality single crystal. The crystal structure of $YbCu_4Ga_8$ is composed of pseudo-Frank–Kasper cages occupying one ytterbium atom in each ring which are shared through the corner along the ab plane, resulting in a three-dimensional network. The magnetic susceptibility of $YbCu_4Ga_8$ investigated in the temperature range 2–300 K showed Curie–Weiss law behavior above 100 K, and the experimentally measured magnetic moment indicates mixed-valent ytterbium. Electrical resistivity measurements show the metallic nature of the compound. At low temperatures, variation of ρ as a function of T indicates a possible Fermi-liquid state at low temperatures.

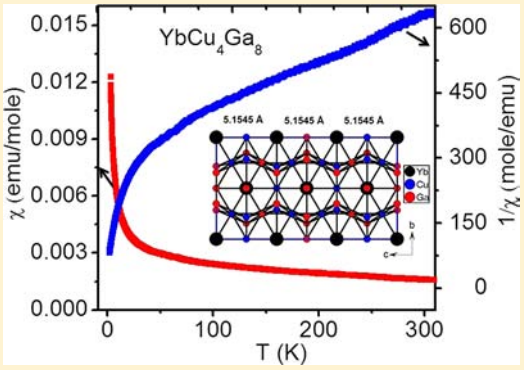

1. INTRODUCTION

Compounds having general formula RET_4X_8 (RE = La–Nd, Sm–Lu, and U; T = Cr, Mn, Fe, Co, Cu, and Ag; X = Al, Ga, and In) have been reported for their interesting physical properties.[1−14] For example, high-temperature antiferromagnetic ordering (T_N) observed in $GdFe_4Al_8$[1] (T_N = 155 K) in addition to the two low-temperature magnetic transitions at T_1 = 21 K and T_2 = 27 K, high-temperature magnetic ordering (163.5 K) in $TbFe_4Al_8$,[2] anisotropic magnetic properties on the single crystals of UFe_4Al_8,[3] and some more compounds are reported in the $REFe_4Al_8$ family.[4−13] The antiferromagnetic–paramagnetic transitions are observed in $GdCr_xAl_{12-x}$ at T_N = 6.50 and 6.75 K for x = 3.5 and 4.0, respectively.[14]

Among the rare earths, the Yb-containing compounds are of particular scientific interest because they can exhibit two energetically similar electronic configurations: the magnetic Yb^{3+} ($4f^{13}$) and the nonmagneticYb^{2+} ($4f^{14}$). In this case, the roles of the 4f electron and 4f hole can be interchanged and Yb-based compounds often crystallize in new structure types.[15−18] Due to these reasons Yb-based compounds exhibit various peculiar properties, such as intermediate valence, heavy fermions, Kondo behavior, unusual magnetism, and superconductivity.[19−26] These properties are generally believed to arise from the strong hybridization leading to interaction between the localized 4f electrons and the delocalized s, p, and d conduction electrons.[27,28]

As per inorganic crystal structure database[29] and Pearson's crystal data,[30] despite a large (ca. 200) number of RET_4X_8 compounds, only a few Yb-based compounds are reported in the 1–4–8 family. Interesting examples are $YbCr_4Al_8$,[31] $YbFe_4Al_8$,[32] $YbMn_4Al_8$,[33] and $YbCu_4Al_8$.[31] All these compounds crystallize in the tetragonal $ThMn_{12}$ structure type (space group $I4/mmm$). $YbCo_{5.4}Ga_{6.6}$[34] and $YbMn_{4.7}Ga_{7.3}$,[35] two gallides, were reported in the same structure type for their phase studies using powder X-ray diffraction, and this motivated us to look for more compounds with first-row transition metals.

Though Cu-based compounds are relatively easy to synthesize using conventional synthesis techniques, only YbCuGa,[36] $YbCu_{5-x}Ga_x$ ($0 \le x \le 2$),[37] $YbCu_xGa_{4-x}$ (x = 1.2 and 0.35),[38] $YbCu_{0.8}Ga_{1.2}$,[39] and $YbCuGa_3$[40] were reported in the Yb–Cu–Ga family, which motivated us to focus on the synthesis of the Ga-rich compounds in the same family.". We noticed that Chan et al. reported the crystal structure and properties of $ThMn_{12}$ structure type $Ln(CuGa)_{12}$ (Ln = Y, Gd–Er, and Yb); here the antiferromagnetic transition was observed at 12.5 K in $Gd(CuGa)_{12}$, 13.5 K in $Tb(CuGa)_{12}$, 6.7 K in $Dy(CuGa)_{12}$, and 3.4 K in $Er(CuGa)_{12}$. However, in $Yb(CuGa)_{12}$ we observed Pauli paramagnetism.[41] We also focused our research to develop the intermetallic chemistry of Yb-based compounds[17,18,42−46] and deeper understanding of the ability of Yb to adopt different or mixed oxidation states. In this paper, we report the synthesis of a new compound $YbCu_4Ga_8$ for the first time which crystallizes in a new structure type, a superstructure derived from the $CeMn_4Al_8$ and $ThMn_{12}$ types. High-quality single crystals of $YbCu_4Ga_8$ were grown using Ga as metal flux. Use of gallium flux has been proved as an excellent tool to produce many novel ternary and quaternary

Received: December 8, 2012
Published: February 7, 2013

   dx.doi.org/10.1021/ic302688n | *Inorg. Chem.* 2013, 52, 2219–2227

intermetallic phases.[47−49] Several new pollygallides with an impressive set of diverse structures and compositions have been synthesized using Ga as solvent.[50−57] The crystal structure of $YbCu_4Ga_8$ was studied using single-crystal X-ray diffraction data, and the Cu/Ga atomic site differentiation was investigated with single-crystal neutron diffraction measurements on a large single crystal. Magnetic susceptibility and electrical resistivity studies were performed on sample obtained by high-frequency induction heating.

2. EXPERIMENTAL SECTION

2.1. Reagents. The following reagents were used as purchased without further purification: Yb (in the form of metal pieces cut from metal chunk, 99.99% Alfa Aesar), Cu (powder, 99.99% Alfa Aesar), and Ga (pieces 99.999% Alfa Aesar).

2.2. Synthesis. *2.2.1. Method I.* High-quality single crystals of $YbCu_4Ga_8$ were obtained by combining 0.1757 g of ytterbium metal, 0.2581 g of copper, and 0.5663 g of gallium, placed in a 9 mm diameter quartz tube, under an inert (argon) atmosphere inside a glovebox, which was flame sealed under vacuum of 10^{-3} Torr, to prevent oxidation during heating. The tube was then placed in a vertically aligned tube furnace and heated to 1000 °C over the period of 5 h, maintained at that temperature for 5 h to allow proper homogenization, followed by cooling to 900 °C in 10 h, and kept there isothermally for 6 days. Finally, the system was allowed to cool to room temperature in 10 h. Unreacted gallium was removed by immersion and sonication in a 2−4 M solution of iodine in dimethylformamide (DMF) over 12−24 h at room temperature. The product was rinsed with hot water and DMF and dried with acetone and ether. Crystals of $YbCu_4Ga_8$ are large (3−4 mm), rod-like obtained in high yield (>90%). A very small amount of Ga metal present in the product was quite unavoidable (detected in powder XRD). Several crystals, which grow as metallic silver rods, were carefully selected for elemental analysis and structure characterization.

2.2.2. Method II. Ytterbium, copper, and gallium elements were mixed in the ideal 1:4:8 atomic ratio and sealed in tantalum ampules under argon atmosphere in an arc-melting apparatus. The tantalum ampules were subsequently placed in a water-cooled sample chamber of an induction furnace (Easy Heat induction heating system, model 7590), first rapidly heated to 180 A (ca. 1300−1450 °C), and kept at that temperature for 20 min. Finally, the reaction was rapidly cooled to room temperature by switching off the power supply. The compound could easily be removed from the tantalum tubes. No reactions with the crucible material could be detected. The compound is in polycrystalline form and light gray in color and was found to be stable in moist air for several months. Weight loss of the final material was found to be less than 1%. Sample obtained from the high-frequency induction heating method was used for property studies.

2.3. Elemental Analysis. Semiquantitative microanalyses were performed on the single crystals obtained from the flux techniques using a scanning Leica 220i electron microscope (SEM) equipped with a Bruker 129 eV energy-dispersive X-ray analyzer (EDS). Data were acquired with an accelerating voltage of 20 kV and in 90 s accumulation time. EDS analysis performed on visibly clean surfaces of the single crystals obtained from the flux method indicated that the atomic composition close to 1:4:8 was in good agreement with the composition obtained from single-crystal data refinement.

2.4. Powder X-ray Diffraction. Phase identity and purity of the $YbCu_4Ga_8$ samples were determined by powder XRD experiments carried out with a Bruker D8 Discover diffractometer using Cu Kα radiation (λ = 1.54187 Å). The experimental powder pattern of $YbCu_4Ga_8$ was compared to the XRD pattern simulated from the single-crystal X-ray structure refinement of $YbCu_4Ga_8$ and found to be in good agreement.

2.5. Single-Crystal X-ray Diffraction. A suitable single crystal of $YbCu_4Ga_8$ was mounted on a thin glass (~0.1 mm) fiber with commercially available super glue. X-ray single-crystal structural data of $YbCu_4Ga_8$ were collected on a Bruker Smart-CCD diffractometer equipped with a normal focus, 2.4 kW sealed tube X-ray source with graphite monochromatic Mo Kα radiation (λ = 0.71073 Å) operating at 50 kV and 30 mA, with ω scan mode. The program SAINT[58] was used for integration of diffraction profiles, and absorption correction were made with the SADABS program.[59] The structure was solved by SHELXS 97[60] and refined by a full matrix least-squares method using SHELXL.[61] Details of the crystallographic data are given in Tables 1−4.

Table 1. Crystal Data and Structure Refinement for $YbCu_4Ga_8$ at 296(2) and 50 K ND data

empirical formula	$YbCu_4Ga_8$	$YbCu_4Ga_8$	$YbCu_4Ga_8$
fw	984.96	984.96	984.96
cryst syst	tetragonal	tetragonal	tetragonal
space group	*I*4/*mmm*	*I*4/*mmm*	*I*4/*mmm*
diffraction method	X-ray	X-ray	neutron
volume	385.93(3) Å^3	1157.91(11) Å^3	1134.7(7) Å^3
Z	2	6	6
a (Å)	8.6529(4)	8.6529(4)	8.600(3)
b (Å)	8.6529(4)	8.6529(4)	8.600(3)
c (Å)	5.1515(1)	15.465(1)	15.342(6)
α (deg)	90.00	90.00	90.00
β (deg)	90.00	90.00	90.00
γ (deg)	90.00	90.00	90.00
density (calcd) (g/cm^3)	8.474	8.473	8.647
absorption coefficient (mm^{-1})	50.071	50.066	51.22
F(000)	867.4	2602.3	610
cryst size (mm^3)	1 × 0.05 × 0.05	0.5 × 0.05 × 0.05	3.00 × 1.00 × 1.00
θ range for data collection (deg)	3.3−32.1	2.6−32.1	9.69−88.00
index ranges	$-12 \le h \le 4$	$-12 \le h \le 4$	$-23 \le h \le 22$
	$-12 \le k \le 12$	$-12 \le k \le 12$	$-22 \le k \le 18$
	$-7 \le l \le 7$	$-23 \le l \le 23$	$-33 \le l \le 36$
no. of reflns collected	1226	3730	3537
no. of independent reflns	218 [R_{int} = 0.0344]	628 [R_{int} = 0.0403]	3537
completeness	100%	99.5%	
	θ = 30.55°	θ = 30.55°	
refinement method	full-matrix least-squares on F^2	full-matrix least-squares on F^2	full-matrix least-squares on F^2
data/restraints/params	218/0/16	628/48/37	3537/48/41
goodness-of-fit	1.191	1.083	1.049
final *R* indices	R_{obs} = 0.024	R_{obs} = 0.042	R_{obs} = 0.059
$I > 2\sigma(I)^a$	wR_{obs} = 0.064	wR_{obs} = 0.136	wR_{obs} = 0.141
R indices	R_{all} = 0.025	R_{all} = 0.074	R_{all} = 0.066
all data	wR_{all} = 0.064	wR_{all} = 0.162	wR_{all} = 0.148
extinction coefficient	0.0077	0.00081(13)	0.000080(11)
largest diff. peak and hole (e·Å^{-3})	2.35 and −2.541	5.951 and −3.578	6.352 and −6.143

$^a R = \Sigma||F_o| - |F_c||/\Sigma|F_o|$, $wR = \{\Sigma[w(|F_o|^2 - |F_c|^2)^2]/\Sigma[w(|F_o|^4)]\}^{1/2}$, and calcd $w = 1/[\sigma^2(F_o^2) + (0.0318P)^2 + 111.1197P]$, where $P = (F_o^2+2F_c^2)/3$.

2.6. Single-Crystal Neutron Diffraction. Neutron diffraction was carried out using the SXD instrument at the ISIS spallation neutron source (Oxfordshire, England).[62] A large crystal of dimensions 1 × 1 × 3 mm^3 was mounted on an aluminum pin with adhesive Al tape inside a top-loading closed-cycle refrigerator in a He exchange gas environment. Five crystal settings were recorded at 50 K with exposure times on the order of 9 h per orientation and data reduced to

dx.doi.org/10.1021/ic302688n | Inorg. Chem. 2013, 52, 2219−2227

Table 2. Atomic Coordinates (×10^4) and Equivalent Isotropic Displacement Parameters (Å^2 × 10^3) for Substructure and Superstructure of $YbCu_4Ga_8$ at 296(2) K with Estimated Standard Deviations in Parentheses

label	Wyckoff site	x	y	z	occupancy	U_{eq}*
substructure						
Yb	2*a*	0	0	0	1	10(3)
Cu	8*f*	2500	2500	2500	1	12(3)
Ga1	8*i*	3463(1)	0	0	1	14(3)
Ga2	8*j*	2847(1)	5000	0	1	23(3)
superstructure						
Yb1	2*a*	0	0	0	1	3(1)
Yb2	4*e*	5000	5000	1664(1)	1	3(1)
Cu1	16*m*	2504(4)	2504(4)	828(2)	1	8(1)
Cu2	8*j*	2840(7)	5000	0	1	6(1)
Ga1	16*n*	5000	1537(3)	1669(2)	1	8(1)
Ga2	8*f*	2500	2500	2500	1	10(1)
Ga3	8*i*	0	3462(6)	0	1	8(1)
Ga4	16*n*	2151(4)	0	1670(2)	1	13(1)
ND data						
Yb1	2*a*	0	0	0	1	1(1)
Yb2	4*e*	5000	5000	1685(7)	1	1(1)
Cu1	16*m*	2534(9)	2534(9)	830(2)	1	3(1)
Cu2	8*j*	3046(2)	5000	0	1	2(1)
Ga1	16*n*	5000	1546(5)	1628(4)	1	4(1)
Ga2	8*f*	2500	2500	2500	1	2(1)
Ga3	8*i*	0	3484(9)	0	1	4(2)
Ga4	16*n*	2259(2)	0	1659(5)	1	4(1)

Table 3. Anisotropic Displacement Parameters (Å^2 × 10^3) for $YbCu_4Ga_8$ at 296(2) K with Estimated Standard Deviations in Parentheses[a]

label	U_{11}	U_{22}	U_{33}	U_{12}	U_{13}	U_{23}
substructure						
Yb	3(3)	3(3)	3(3)	0	0	0
Cu	8(4)	8(4)	2(1)	1(1)	1(1)	0
Ga1	5(1)	6(1)	11(5)	0	0	0
Ga2	29(7)	6(1)	5(1)	0	0	0
superstructure						
Yb1	3(1)	3(1)	4(1)	0	0	0
Yb2	2(1)	2(1)	4(1)	0	0	0
Cu1	8(1)	5(1)	4(1)	0	0	0
Cu2	13(2)	5(2)	4(1)	0	2(1)	2(1)
Ga1	6(1)	6(1)	11(1)	0	0	0
Ga2	10(1)	10(1)	9(1)	0	−1(1)	−1(1)
Ga3	7(2)	6(2)	10(2)	0	0	0
Ga4	22(2)	8(1)	8(1)	0	0	0
ND data						
Yb1	1(1)	1(1)	1(1)	0	0	0
Yb2	1(1)	1(1)	1(1)	0	0	0
Cu1	3(1)	3(1)	2(1)	−1(1)	0	0
Cu2	4(1)	2(1)	1(1)	0	0	0
Ga1	3(1)	2(1)	6(1)	0	0	0
Ga2	2(1)	2(1)	2(1)	−1(1)	0	0
Ga3	5(1)	4(2)	4(2)	0	0	0
Ga4	6(1)	2(3)	3(1)	0	2(1)	0

[a]The anisotropic displacement factor exponent takes the form $-2\pi^2[h^2a^{*2}U_{11} + ... + 2hkabU_{12}]$.

Table 4. Selected Bond Lengths [Angstroms] for $YbCu_4Ga_8$ at 296(2) K with Estimated Standard Deviations in Parentheses

label	distances	label	distances
Cu1—Cu1	2.589(3)	Ga2—Ga2	2.643(7)
Cu1—Cu2	2.537(3)	Ga3—Ga3	2.659(7)
Cu2—Cu2	2.636(6)	Ga3—Ga4	2.811(3)
Cu1—Ga2	2.571(16)	Ga4—Ga4	2.634(4)
Cu1—Ga3	2.656(2)	Ga4—Ga3	2.797(4)
Cu1—Ga1	2.646(2)	Ga4—Ga2	2.539(12)
Cu2—Ga2	2.535(13)	Yb1—Cu2	3.180(2)
Cu2—Ga3	2.798(4)	Yb2—Cu2	3.183(3)
Cu1—Ga4	2.531(3)	Yb2—Ga1	2.995(19)
Cu2—Ga1	2.809(3)	Yb1—Ga3	2.997(4)
Ga1—Ga1	2.661(4)	Yb2—Ga2	3.318(7)
Ga1—Ga2	2.655(14)	Yb2—Ga4	3.182(3)
Ga1—Ga4	2.800(2)	Yb1—Ga4	3.175(2)
Ga1—Ga4	2.827(3)		

structure factors using the locally available program SXD2001.[63] Sample absorption was found negligible and did not influence the final result. The structure was solved by SHELXS 97[60] and refined by a full matrix least-squares method using SHELXL.[61]

2.7. Magnetic Measurements. Magnetic measurements of $YbCu_4Ga_8$ were carried out on a Quantum Design MPMS-SQUID magnetometer. Measurements were performed on polycrystals, which were ground and screened by powder XRD to verify phase identity and purity. Temperature-dependent data were collected for field-cooled mode (FC) between 2 and 300 K in an applied field (H) of 1000 Oe. Magnetization data were also collected for $YbCu_4Ga_8$ at 2 and 300 K with field sweeping from −55 000 to 55 000 Oe.

2.8. Electrical Resistivity. Resistivity measurements were performed in 1 T field on $YbCu_4Ga_8$ with a conventional ac four-probe setup. Four very thin copper wires were glued to the pellet using a strongly conducting silver epoxy paste. Data were collected in the range 3−300 K using a commercial Quantum Design Physical Property Measurement System (QD-PPMS). Results were reproducible for several batches.

dx.doi.org/10.1021/ic302688n | Inorg. Chem. 2013, 52, 2219−2227

3. RESULTS AND DISCUSSION

3.1. Reaction Chemistry. Compound $YbCu_4Ga_8$ was obtained from reactions of Yb/Cu/Ga in liquid gallium which acted as reactive solvent and formed a new compound $YbCu_4Ga_8$. The gray rod-shaped single crystal of $YbCu_4Ga_8$ obtained from the flux reaction is shown in Figure 1. $YbCu_4Ga_8$

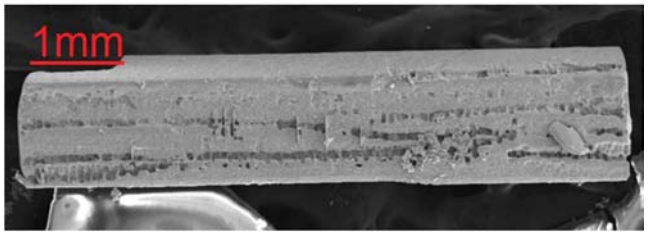

Figure 1. SEM image of a typical $YbCu_4Ga_8$ single crystal grown from Ga flux.

is stable in air, and no decomposition was observed even after several months. A high-quality single crystal was used to collect the XRD data and refined the crystal structure within the $CeMn_4Al_8$ type, and different lattice parameters are $a = b = 8.649(4)$ Å and $c = 5.1484(3)$ Å. Elemental analysis of this compound with SEM/EDS gave the atomic composition 1:4:8, which is in excellent agreement with the results obtained from single-crystal refinement. The XRD pattern of the powdered sample is in good agreement with the simulated pattern obtained from single-crystal data. However, a close look at the powder data (Supporting Information) showed additional peaks indicating a possible superstructure reflection or minor impurity phase. Then the data was refined within a new structure type, a superstructure of the $CeMn_4Al_8$ type, and the lattice parameters obtained are $a = b = 8.6529(4)$ Å and $c = 15.465(1)$ Å. The superstructure reflections are clearly visible in the experimental powder XRD pattern of $YbCu_4Ga_8$ as shown in the Supporting Information.

This was further proved by the synthesis of pure $YbCu_4Ga_8$ compound using conventional high-frequency induction method as described in Method II. After a synthesis method was established for $YbCu_4Ga_8$ other first-row transition metals also employed a similar reaction condition in order to produce more members in the YbT_4Ga_8 (Ni, Co, and Ag) family but was not successful.

3.2. Structure Refinement of $YbCu_4Ga_8$. The crystal structure of $YbCu_4Ga_8$ was refined using SHELXL-97 (full-matrix least-squares on F^2)[60] with anisotropic atomic displacement parameters for all atoms. As a check for the correct composition, occupancy parameters were refined in a separate series of least-squares cycles. Single crystals of $YbCu_4Ga_8$ from different synthesis batches were used for data collection. In the first step of refinement on the single-crystal data collected shows that $YbCu_4Ga_8$ crystallizes in a body-centered tetragonal lattice ($I4/mmm$) within the $CeMn_4Al_8$-type structure, and lattice constants are $a = b = 8.6529(4)$ Å and $c = 5.155(3)$ Å. This refinement resulted in four crystallographic positions in the $YbCu_4Ga_8$ structure: one ytterbium atom occupies a 2*a* site, one copper atom occupies a 8*f* site, and two gallium atoms occupy 8*i* and 8*j* sites. During isotropic refinement of $YbCu_4Ga_8$, it was observed that the highest difference peak and deepest hole are 12 and −3.6, respectively. Our attempts to refine the mixed positions of Cu and Ga also did not solve the highest difference peak and deepest hole. In addition, the anisotropic displacement parameter U_{33} of all four positions

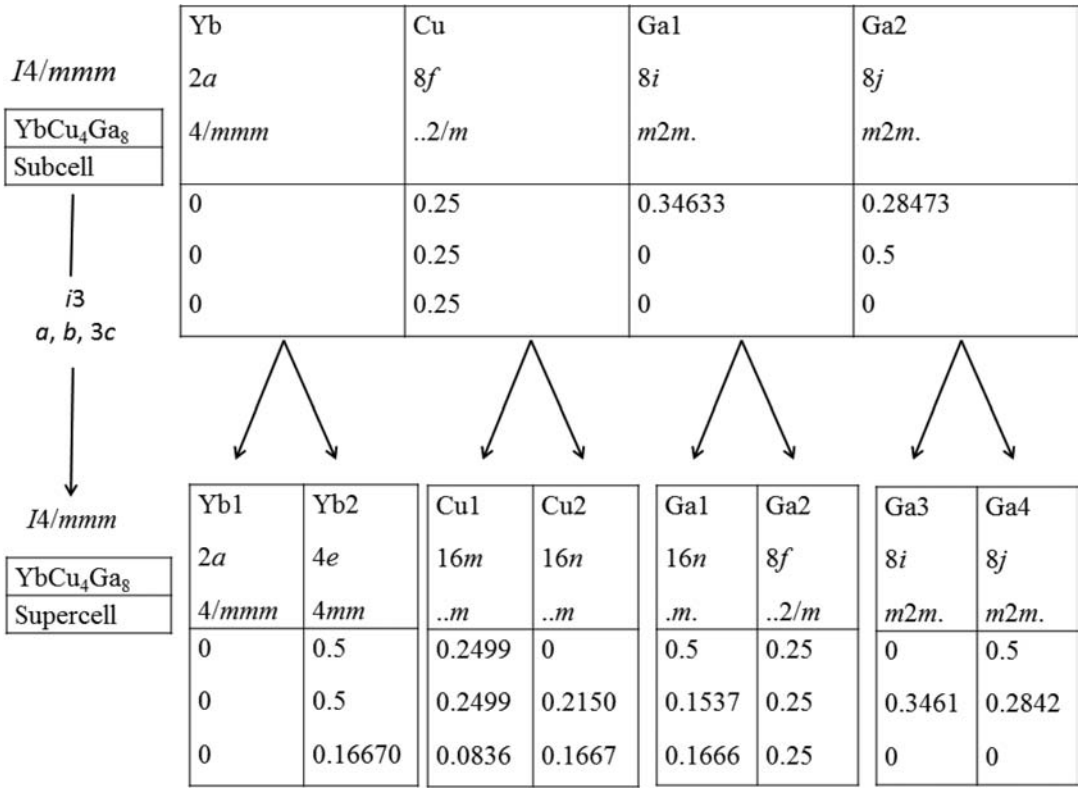

Figure 2. Group−subgroup scheme in the Bärnighausen formalism for the subcell and superstructure of $YbCu_4Ga_8$. Indices for the isomorphic (i) transition and unit cell transformations are given. Evolution of the atomic parameters is shown at the right.

dx.doi.org/10.1021/ic302688n | Inorg. Chem. 2013, 52, 2219−2227

was slightly larger. All these facts indicated that the $YbCu_4Ga_8$ compound crystallizes in the superstructure, and our refinement indeed confirms this with a stable refinement with a tripling of the *c* axis.

In the second step we considered the superstructure reflections and refined the structure in the same space group *I*4/*mmm* within the superstructure of the $CeMn_4Al_8$-type structure, and the lattice parameters are $a = b = 8.6529(4)$ Å and $c = 15.465(1)$ Å. In this refinement, there are eight crystallographic positions in the $YbCu_4Ga_8$ superstructure of which two ytterbium atoms occupy 2*a* and 4*e* sites, two copper atoms occupy 8*i* and 16*m*, and four gallium atoms occupy two 16*n*, 8*j*, and 8*f* sites. Final refinement is quite stable, and the overall stoichiometry obtained from the refinement is $YbCu_4Ga_8$. Owing to the small contrast between Cu and Ga, the assignment of the sites was further checked using single-crystal neutron diffraction. The sites were initially assigned to be of type Ga and the occupancy refined one site at a time to decide whether it was occupied by Ga or Cu.

Data collection and structure refinement for $YbCu_4Ga_8$ using both X-ray and neutron are listed in Table 1. Standard atomic positions and isotropic atomic displacement parameters of this compound are collected in Table 2. Anisotropic displacement parameters and important bond lengths are listed in Tables 3 and 4, respectively. The group−subgroup scheme in the Bärnighausen formalism[64−66] for the subcell and the superstructure of $YbCu_4Ga_8$ is given in Figure 2. Further information on - structure refinements is available from Fachinformationszentrum Karlsruhe, D-76344 Eggenstein-Leopoldshafen (Germany), by quoting Registry Nos. CSD-424999 (Substructure), CSD-425503 (Superstructure XRD), and CSD-425502 (ND).

3.3. Crystal Chemistry of $YbCu_4Ga_8$. The crystal structure of $YbCu_4Ga_8$ along the *c* axis is shown in Figure 3A. $YbCu_4Ga_8$ crystallizes in the tetragonal superstructure of the $CeMn_4Al_8$ type (space group *I*4/*mmm*), which is an ordered superstructure of the $ThMn_{12}$ type. The crystal structure of $YbCu_4Ga_8$ is composed of 8 Cu atoms and 12 Ga atoms, forming $[Cu_8Ga_{12}]$ cages occupying one ytterbium atom in each ring to form a stable structure. These cages are shared through the corner Cu linkage along the *ab* plane, resulting in a three-dimensional network. Bonds to the Yb atoms have been omitted to emphasize the 3D $[Cu_4Ga_8]$ framework and its channels (Figure 3B). The tripling of the *c* axis in the subcell of the $YbCu_4Ga_8$ structure ($CeMn_4Al_8$ type) is shown in Figure 4A. The compound contains two layers: one distorted slab contains Cu and Ga atoms (Figure 4B), and a planar layer contains all three elements (Figure 4D). These two layers are interconnected through the bonds between Cu and Ga atoms, forming a stable three-dimensional structure. In the distorted layer, Cu and Ga atoms form a 2-dimensional sheet that extends in the *bc* plane (Figure 4A) and is capped by Cu and Ga atoms alternatively above and below this plane, thus forming a puckered overall layer (Figure 4C). The planar layer, on the other hand, forms one-dimensional (1D) cis and trans infinite zigzag chains of Cu and Ga atoms propagating along the *c* axis as shown in Figure 3D. These cis and trans chains are interconnected through the Ga−Ga bonds, forming one-dimensional hexagons which are separated by ordered Yb atoms.

The average Cu−Cu bond distance in the $YbCu_4Ga_8$ crystal structure 2.563(3) Å is close to the atomic radii of Cu−Cu distance (2.560 Å) observed in $YbCu_4Al_8$[31] and exactly matching with the theoretical distance of 2.56 Å.[67] The

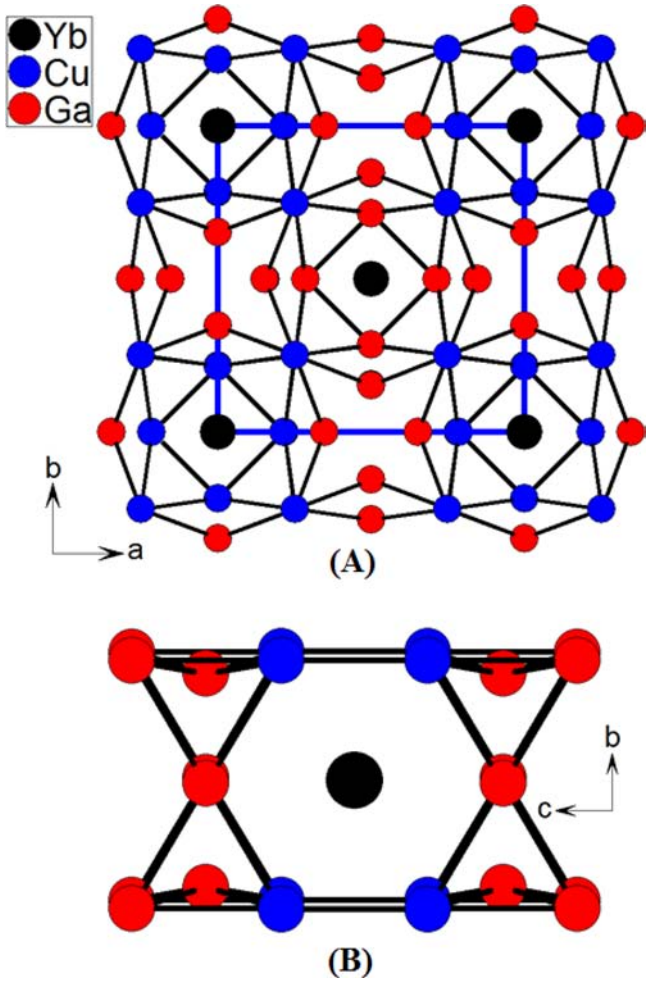

Figure 3. (A) Crystal structure of $YbCu_4Ga_8$ as viewed along the *c* axis; unit cell is outlined as blue solid lines. (B) Cu_4Ga_8 framework shown along the [010] direction with an Yb atom sandwich in between them.

shortest distance of Yb−Ga of 2.996(7) Å is smaller than the calculated distances of Yb^{2+}−Ga (3.09 Å)[68,69] and larger than Yb^{3+}−Ga (2.92 Å),[68,69] suggesting mixed valency or intermediate valency of Yb atoms in $YbCu_4Ga_8$. However, both Yb1−Ga and Yb2−Ga short distances are similar, ruling out the mixed valency; instead, $YbCu_4Ga_8$ is an intermediate-valent compound. The shortest distance between Yb and Cu atoms, 3.178(2) Å, is close to the radii of Yb−Cu distance (3.176 Å) observed in $YbCu_2Si_2$[70] but slightly shorter than the theoretical distance of 3.19 Å of Yb^{2+}−Cu.

The local coordination environments of all atoms in the crystal structure of $YbCu_4Ga_8$ are presented in Figure 5. The coordination environments of the Yb1 and Yb2 atoms are similar and formed as cages of 20 atoms $Cu_{16}Ga_4$ and Cu_8Ga_{12}, respectively. The coordination environments for the Cu1 and Cu2 atoms are similarly composed as a cuboctahedran of $[Yb_2Cu_3Ga_7]$ and $[Yb_2Cu_4Ga_6]$, respectively. Ga1 and Ga3 have a similar sphere composed of a 14-vertex Frank−Kasper cage of $[YbCu_5Ga_8]$ and $[YbCu_6Ga_7]$, respectively. Ga2 and Ga4 atoms also have similar coordination environments composed as an icosahedron of $[Yb_2Cu_6Ga_4]$ and $[Yb_2Cu_4Ga_6]$, respectively.

3.4. Physical Properties. *3.4.2. Magnetism.* Magnetic susceptibility measurements were made on a polycrystalline

dx.doi.org/10.1021/ic302688n | Inorg. Chem. 2013, 52, 2219−2227

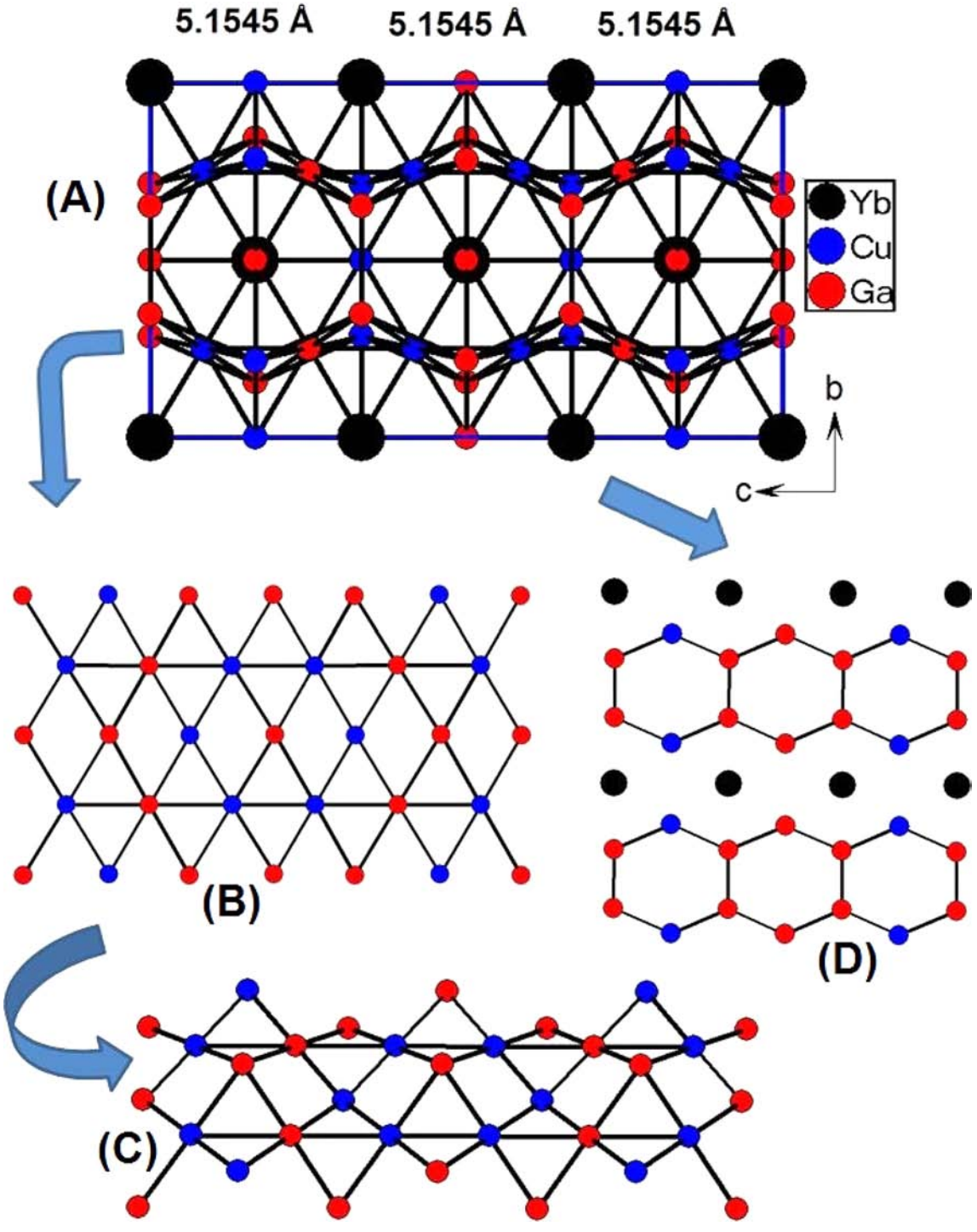

Figure 4. (A) Crystal structure of $YbCu_4Ga_8$ as viewed along the *a* axis. (B) Projection of the fragment $[Cu_xGa_y]$. (C) Rotated view of the $[Cu_xGa_y]$ slab where the puckered form of the layer is emphasized. (D) Projection of the planar layer of $YbCu_{4-x}Ga_{8-y}$.

sample of $YbCu_4Ga_8$ obtained from high-frequency induction heating synthesis. The temperature-dependent molar magnetic susceptibility (χ_m) and inverse susceptibility ($1/\chi_m$) of $YbCu_4Ga_8$ at an applied field of 10 000 Oe are shown in Figure 6. The magnetic susceptibility, also measured on single crystals in two orientations, one being parallel to the applied magnetic field (marked as H ∥ *c* axis) and other being perpendicular to the field (marked as H ⊥ *c* axis) (shown in the Supporting Information, Figure S3). In all measurements, χ increases gradually with increasing temperature with no magnetic ordering down to 2 K but the susceptibility slightly increases at lower temperature with increasing field, which is normal for rare-earth-based intermetallics.[71−73] The inverse susceptibility curve obeys modified Curie−Weiss law, $\chi = C/(T - \theta) + \chi_0$ (χ_0 = 0.00519 emu/mol), in the range of 100−290 K with an effective magnetic moment of 2.77 μ_B/Yb atom, suggesting the mixed-valent or intermediate-valent nature of Yb atoms. The estimated experimental μ_{eff} value is about 60% of that expected for a free ion Yb^{3+} moment (4.56 μ_B/Yb). However, the calculated magnetic moment for Yb in $YbCu_4Ga_8$

dx.doi.org/10.1021/ic302688n | *Inorg. Chem.* 2013, 52, 2219−2227

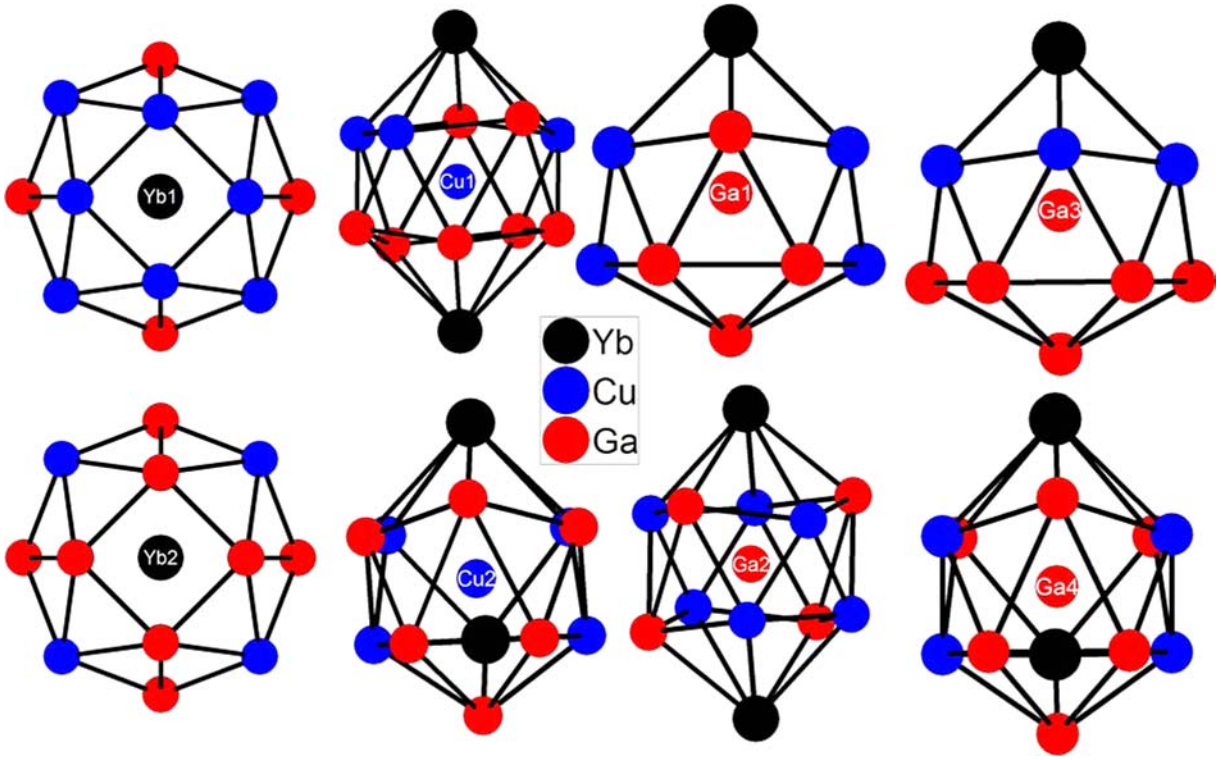

Figure 5. Coordination sphere of all atoms in the crystal structure of $YbCu_4Ga_8$.

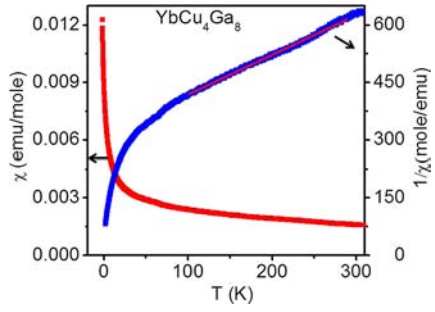

Figure 6. Temperature dependence of the modified magnetic susceptibility (χ_m) and reciprocal magnetic susceptibility ($1/\chi_m$) of the $YbCu_4Ga_8$. Red straight line shows the temperature range where the modified Curie–Weiss law was applied to calculate the magnetic moment.

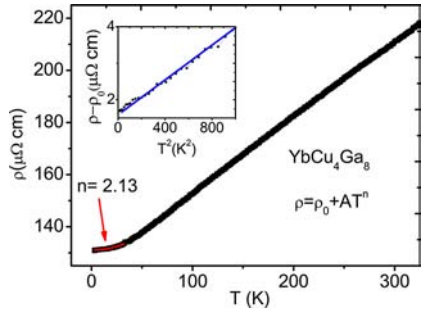

Figure 7. Resistivity (ρ) measured as a function of temperature. Low-temperature data have been fitted to the power law $\rho = \rho_0 + AT^n$. Values obtained from the fit are shown in inset.

(40% Yb^{2+}) is close to the value observed for Yb in $YbLiGe_2$[74] and Yb_5Ge_4[75] compounds. Drake et al. already pointed out the negligible temperature dependence of the magnetic susceptibility and speculated the mixed valence of Yb in $Yb(CuGa)_{12}$.[41] Felner and Nowik studied the magnetic properties of other prototypes YbT_4Al_8 (T = Cr, Mn, Fe, and Cu) in detail and observed the mixed-valent behavior of Yb in the $YbCr_4Al_8$ and $YbCu_4Al_8$ compounds as they exhibit temperature-independent paramgnetism and positive Curie–Weiss temperature, and later it was confirmed by ^{170}Yb Mössbauer spectroscopy.[27] On the other hand, in $YbMn_4Al_8$ and $YbFe_4Al_8$ the Yb ion exists as divalent and trivalent, respectively.

3.4.2. Electrical Resistivity. The normal state temperature-dependent resistivity of $YbCu_4Ga_8$ is shown in Figure 7, continuously decreasing linearly with decreasing temperature, typical for metallic systems[76,77] but without any long-range magnetic ordering. The resistivity value of $YbCu_4Ga_8$ of 220 $\mu\Omega$·cm at room temperature is comparable to the resistivity of $Yb_5Ir_4Ge_{10}$ (220 $\mu\Omega$·cm).[78]

At low temperature in the range of 3–30 K, the $\rho(T)$ data can be fitted to the power law function, $\rho = \rho_0 + AT^n$, where ρ_0 is the residual resistivity expressed in units of Ω·cm (ρ_0 is 131 $\mu\Omega$·cm), where A and n are the fitting parameters. According to Fermi-liquid theory, at low temperatures, the resistivity varies as $\rho = \rho_0 + AT^2$. Experimentally it has been observed that when electron–electron scattering dominates over electron–phonon scattering, $\rho \alpha T^2$. The value obtained from the fit is slightly larger than 2 in $YbCu_4Ga_8$, which is the case for systems exhibiting Fermi-liquid state.[79,80] In order to verify Fermi liquid behavior, resistivity data is plotted as $(\rho - \rho_0)$ vs T^2 as inset to Figure 7. For $YbCu_4Ga_8$, linearity in the data indicates a probable Fermi-liquid behavior in this compound at low temperatures.

dx.doi.org/10.1021/ic302688n | Inorg. Chem. 2013, 52, 2219–2227

4. CONCLUDING REMARKS

High-quality single crystals of $YbCu_4Ga_8$ were obtained from the metal flux technique, and the crystal structure of $YbCu_4Ga_8$ was studied using single-crystal X-ray diffraction. $YbCu_4Ga_8$ crystallizes in a new structure type, a superstructure of $CeMn_4Al_8$. The metal flux technique has been proved as a vital synthesis method to obtain novel compounds within new structure types. The magnetic susceptibility of $YbCu_4Ga_8$ following modified Curie–Weiss law in the temperature range of 100–300 K, and the estimated experimental μ_{eff} value is 60% of Yb^{3+} compared to the theoretical value of 4.56 μ_B/Yb. Our detailed bond analysis confirmed that Yb atoms of $YbCu_4Ga_8$ are in the intermediate valent state. The electrical resistivity physical measurements of $YbCu_4Ga_8$ suggest a possible Fermi-liquid ground state at low temperature as $\rho \alpha T^2$.

■ ASSOCIATED CONTENT

Ⓢ Supporting Information

Crystallographic information files (CIF), powder XRD comparison, and magnetic susceptibility plot on single crystals. This material is available free of charge via the Internet at http://pubs.acs.org.

■ AUTHOR INFORMATION

Corresponding Author

*Phone: 080-22082998. Fax: 080-22082627. E-mail: sebastiancp@jncasr.ac.in.

Notes

The authors declare no competing financial interest.

■ ACKNOWLEDGMENTS

We thank Prof. C. N. R. Rao for his support and guidance. Financial support from JNCASR, DST (Grant SR/S2/RJN-24/2010), and Sheikh Saqr Laboratory is gratefully acknowledged. U.S. thanks CSIR for a research fellowship, and S.C.P. thanks DST for a Ramanujan Fellowship.

■ REFERENCES

(1) Angst, M.; Kreyssig, A.; Janssen, Y.; Kim, J. W.; Tan, L.; Wermeille, D.; Mozharivskyij, Y.; Kracher, A.; Goldman, A. I.; Canfield, P. C. *Phys. Rev. B* **2005**, *72*, 174407–174420.

(2) Buschow, K. H. J.; Van der Kraan, A. M. *J. Phys. (Paris)* **1978**, *F 8*, 921.

(3) Godinho, M.; Bonfait, G.; Gorqalves, A. P.; Almeida, M.; Spirlet, J. C. *J. Magn. Magn. Mater.* **1995**, *140–144*, 1417–1418.

(4) Zarechnyuk, O. S.; Krypyakevych, P. I. *Sov. Phys. Crystallogr.* **1962**, *7*, 436–446; *Kristallografiya* **1962**, *7*, 543–554.

(5) Gladyshevskii, E. I.; Krypyakevych, P. I.; Teslyuk, M. Y.; Zarechnyuk, O. S.; Kuz'ma, Y. B. *Sov. Phys. Crystallogr* **1961**, *6*, 207–208; *Kristallografiya* **1961**, *6*, 267–268.

(6) Klesnar, H. P.; Rogl, P. *J. Mater. Res.* **1991**, *6*, 53–56.

(7) Felner, I. *J. Less-Common Met.* **1980**, *72*, 241–249.

(8) Felner, I.; Nowik, I. *J. Phys. Chem. Solids* **1978**, *39*, 951–956.

(9) Schäfer, W.; Grönefeld, M.; Will, G.; Gal, J. *Mater. Sci. Forum* **1988**, *27–28*, 243–248.

(10) Schäfer, W.; Will, G. *J. Less-Common Met.* **1983**, *94*, 205–212.

(11) Vivchar, O. I.; Zarechnyuk, O. S.; Ryabov, V. R. *Dopov. Akad. Nauk Ukr. RSR (Ser. A)* **1973**, 159–161.

(12) Zarechnyuk, O. S.; Vivchar, O. I.; Ryabov, V. R. *Visn. L'viv. Derzh. Univ. (Ser. Khim.)* **1972**, 14–16.

(13) Yanson, T. I.; Manyako, M. B.; Bodak, O. I.; Cerny, R.; Pacheco, J. V.; Yvon, K. *Z. Kristallogr. (New Cryst. Struct.)* **1997**, 212–505.

(14) Verbovytsky, Y.; Latka, K.; Pacyna, A. W.; Tomala, K. *J. Alloys Compd.* **2007**, *438*, L12–L15.

(15) Peter, S. C.; Chondroudi, M.; Malliakas, C. D.; Balasubramanian, M.; Kanatzidis, M. G. *J. Am. Chem. Soc.* **2011**, *133*, 13840–13843.

(16) Park, S. M.; Kim, S. J.; Kanatzidis, M. G. *J. Solid State Chem.* **2004**, *177*, 2867–2874.

(17) Chondroudi, M.; Balasubramanian, M.; Welp, U.; Kwok, W.; Kanatzidis, M. G. *Chem. Mater.* **2007**, *19*, 4769–4775.

(18) Peter, S. C.; Salvador, J.; Martin, J. B.; Kanatzidis, M. G. *Inorg. Chem.* **2010**, *49*, 10468–10474.

(19) Kindler, B.; Finsterbusch, D.; Graf, R.; Ritter, F. *Phys. Rev. B* **1994**, *50*, 704–707.

(20) Bauer, E. *Adv. Phys.* **1991**, *40*, 417.

(21) Wachter, P. *Handbook on the Physics and Chemistry of Rare Earths*; Elsevier Science: Amsterdam, 1994; p 177.

(22) Matsumoto, Y.; Nakatsuji, S.; Kuga, K.; Karaki, Y.; Horie, N.; Shimura, Y.; Sakakibara, T.; Nevidomskyy, A. H.; Coleman, P. *Science* **2011**, *331*, 316–319.

(23) Ernst, S.; Kirchner, S.; Krellner, C.; Geibel, C.; Zwicknagl, G.; Steglich, F.; Wirth, S. *Nature* **2011**, *474*, 362–366.

(24) Stockert, O.; Arndt, J.; Faulhaber, E.; Geibel, C.; Jeevan, H. S.; Kirchner, S.; Loewenhaupt, M.; Schmalzl, K.; Schmidt, W.; Si, Q.; Steglich, F. *Nat. Phys.* **2011**, *7*, 119–124.

(25) Hausermannberg, L. S.; Shelton, R. N. *Phys. Rev. B* **1987**, *35*, 6659–6664.

(26) Braun, H. F.; Segre, C. U. *Solid State Commun.* **1980**, *35*, 735–738.

(27) Lawrence, J. M.; Riseborough, P. S.; Park, R. D. *Rep. Prog. Phys.* **1981**, *44*, 1–84.

(28) Fisk, Z.; Hess, D. W.; Pethick, C. J.; Pines, D.; Smith, J. L.; Thomson, J. D.; Willis, J. O. *Science* **1988**, *239*, 33–42.

(29) Bergerhoff, G.; Brown, I. D. In *Crystallographic Databases*; Allen, F. H. et al., Eds.; International Union of Crystallography: Chester, 1987.

(30) Villars, P.; Cenzual, K. *Pearson's Crystal Data-Crystal Structure Database for Inorganic Compounds*, Release 2010/11; ASM International: Materials Park, OH, 2010.

(31) Felner, I.; Nowik, I. *J. Phys. Chem. Solids* **1979**, *40*, 1035–1044.

(32) Drulis, H.; Gaczynski, P.; Iwasieczko, W.; Suski, W.; Kotur, B. Y. *Solid State Commun.* **2002**, *123*, 391–394.

(33) Buschow, K. H. J.; Van Vucht, J. H. N.; Van Den Hoogenhof, W. W. *J. Less-Common Met.* **1976**, *50*, 145–150.

(34) Chernyak, B. I.; Gladyshevskii, R. E. *Tezizy Dokl. Vses. Konf. Kristallokhim. Intermet. Soeden. 4th (Lvov)* **1983**, 47–48.

(35) Markiv, V. Y.; Belyavina, N. N.; Karpenko, V. A.; Karpenko, A. A. *Dopov. Akad. Nauk Ukr. RSR (Ser. A)* **1985**, 9–76.

(36) (a) Adroja, D. T.; Malik, S. K.; Padalia, P. D.; Bhatia, S. N.; Walia, R.; Vijayaraghavan, R. *Phys. Rev. B* **1990**, *42*, 2700–2703. (b) Adroja, D. T.; Rainford, B. D.; Malik, L. E.; Malik, S. K. *Physica B* **1997**, *230–232*, 282–285.

(37) (a) Adroja, D. T.; Malik, S. K.; Padalia, B. D.; Vijayaraghavan, R. *J. Phys. C: Solid State Phys.* **1987**, *20*, L307–L310. (b) He, J.; Ling, G.; Jiao, Z. *Physica B* **2001**, *301*, 196–202. (c) Bauer, E.; Tuan, L.; Hauser, R.; Gratz, E.; Holubar, T.; Hilscher, G.; Michor, G.; Perthold, W.; Godart, C.; Alleno, E.; Hiebl, K. *Phys. Rev. B* **1995**, *52*, 4327–4335.

(38) (a) Markiv, V. Y.; Shevchenko, I. P.; Belyavina, N. N.; Kuzmenko, P. P. *Dopov. Akad. Nauk Ukr. RSR (Ser. A)* **1985**, 7–76. (b) Grin, Y.; Ellner, M.; Hiebl, K.; Rogl, P. *J. Alloys Compd.* **1993**, *196*, 207–212.

(39) Markiv, V. Y.; Belyavina, N. N.; Zhunkovskaya, T. I. *Dopov. Akad. Nauk Ukr. RSR (Ser. A)* **1982**, 2–80.

(40) Subbarao, U.; Peter, S. C. *Cryst. Growth Des.* DOI: 10.1021/cg301765f

(41) Drake, B. L.; Capan, C.; Cho, J. Y.; Nambu, Y.; Kuga, K.; Xiong, Y. M.; Karki, A. B.; Nakatsuji, S.; Adams, P. W.; Young, D. P.; Chan, J. Y. *J. Phys.: Condens. Matter* **2010**, *22*, 066001–066014.

(42) Zhuravleva, M. A.; Kanatzidis, M. G. *J. Solid State Chem.* **2003**, *173*, 280–292.

(43) Subbarao, U.; Peter, S. C. *Inorg. Chem.* **2012**, *51*, 6326−6332.
(44) (a) Peter, S. C.; Kanatzidis, M. G. *J. Solid State Chem.* **2010**, *183*, 2077−2081. (b) Margadonna, S.; Prassides, K.; Chondroudi, M.; Salvador, J. R.; Kanatzidis, M. G. *Chem. Commun.* **2005**, 5754−5756. (c) Wu, X. N.; Francisco, M.; Rak, Z.; Bakas, T.; Mahanti, S. D.; Kanatzidis, M. G. *J. Solid State Chem.* **2008**, *181*, 3269−3277. (d) Chondroudi, M.; Peter, S. C.; Malliakas, C. D.; Balasubramanian, M.; Li, Q.; Kanatzidis, M. G. *Inorg. Chem.* **2011**, *50*, 1184−1193.
(45) Peter, S. C; Disseler, S. M.; Svensson, J. N.; Carretta, P.; Graf, M. J. *J. Alloys Compd.* **2011**, *516*, 126−133.
(46) Zhuravleva, M. A.; Salvador, J.; Bilc, D.; Mahanti, S. D.; Ireland, J.; Kannewurf, C. R.; Kanatzidis, M. G. *Chem.—Eur. J.* **2004**, *10*, 3197−3208.
(47) Kanatzidis, M. G.; Pöttgen, R.; Jeitschko, W. *Angew. Chem., Int. Ed.* **2005**, *44*, 6996−7023.
(48) Tobash, P. H.; Bobev, S.; Thompson, J. D.; Sarrao, J. L. *J. Alloys Compd.* **2009**, *488*, 533−537.
(49) Bobev, S.; Hullmann, J.; Harmening, T.; Pöttgen, R. *Dalton Trans.* **2010**, *39*, 6049−6055.
(50) Chen, X. Z.; Larson, P.; Sportouch, S.; Brazis, P.; Mahanti, S. D.; Kannewurf, C. R.; Kanatzidis, M. G. *Chem. Mater.* **1999**, *11*, 75−83.
(51) Chen, X. Z.; Small, P.; Sportouch, S.; Zhuravleva, M.; Brazis, P.; Kannewurf, C. R.; Kanatzidis, M. G. *Chem. Mater.* **2000**, *12*, 2520−2522.
(52) Zhuravleva, M. A.; Bilc, D.; Pcionek, R. J.; Mahanti, S. D.; Kanatzidis, M. G. *Inorg. Chem.* **2005**, *44*, 2177−2188.
(53) Schluter, M.; Jeitschko, W. *Inorg. Chem.* **2001**, *40*, 6362−6368.
(54) Zhuravleva, M. A.; Kanatzidis, M. G. *Inorg. Chem.* **2008**, *47*, 9471−9477.
(55) Zhuravleva, M. A.; Wang, X. P.; Schultz, A. J.; Bakas, T.; Kanatzidis, M. G. *Inorg. Chem.* **2002**, *41*, 6056−6061.
(56) Menard, M. C.; Drake, B. L.; McCandless, G. T.; Thomas, K. R.; Hembree, R. D.; Haldolaarachchige, N.; DiTusa, J. F.; Young, D. P.; Chan, J. Y. *Eur. J. Inorg. Chem.* **2011**, *26*, 3909−3919.
(57) Gray, D. L.; Francisco, M. C.; Kanatzidis, M. G. *Inorg. Chem.* **2008**, *47*, 7243−7248.
(58) *SAINT*, 6.02 ed.; Bruker AXS: Madison, WI, 1999.
(59) Sheldrick, G. M. *SADABS, Empirical Absorption Correction Program*; University of Göttingen: Göttingen, Germany, 1997.
(60) Sheldrick, G. M. *Acta Crystallogr.* **2008**, *A64*, 112−122.
(61) *SHELXTL 5.10*; Bruker Analytical X-ray Systems, Inc.: Madison, WI, 1997.
(62) Keen, D. A.; Gutmann, M. J.; Wilson, C. C. *J. Appl. Crystallogr.* **2006**, *39*, 714−722.
(63) Gutmann, M. J. *SXD2001*; ISIS Facility, Rutherford Appleton Laboratory: Oxfordshire, England, 2005.
(64) Bärnighausen, H. *Commun. Math. Chem.* **1980**, *9*, 139−175.
(65) Bärnighausen, H.; Müller, U. Symmetriebeziehungen zwischen den Raumgruppen als Hilfsmittel zur straffen Darstellung Von Strukturzusammenha ïgen in der Kristallchemie; University of Karlsruhe and University/GH Kassel: Karlsruhe, Germany, 1996.
(66) Müller, U. *Z. Anorg. Allg. Chem.* **2004**, *630*, 1519−1537.
(67) Vanýsek, P. Electrochemical Science and Technology of Copper. *Proceedings of the International Symposium*; The Electrochemical Society, 2002.
(68) Sanderson, R. T. *J. Am. Chem. Soc.* **1983**, *105*, 2259−2261.
(69) Allen, F. H.; Kennard, O.; Watson, D. G.; Brammer, L.; Orpen, A. G.; Taylor, R. *J. Chem. Soc., Perkin Trans.* **1987**, *2*, S1−S19.
(70) Rieger, W.; Parthé, E. *Monatsh. Chem.* **1969**, *100*, 444−454.
(71) Peter, S. C.; Rayaprol, S.; Francisco, M. C.; Kanatzidis, M. G. *Eur. J. Inorg. Chem.* **2011**, 3963−3968.
(72) Peter, S. C.; Eckert, H.; Fehse, C.; Wright, J. P.; Attfield, J. P.; Johrendt, D.; Rayaprol, S.; Hoffmann, R. D.; Pöttgen, R. *J. Solid State Chem.* **2006**, *179*, 2376−2385.
(73) Chondroudi, M.; Peter, S. C.; Malliakas, C. D.; Balasubramanian, M.; Li, Q.; Kanatzidis, M. G. *Inorg. Chem.* **2011**, *50*, 1184−1193.
(74) Iyer, A. K.; Peter, S. C. *Eur. J. Inorg. Chem.* **2012**, *11*, 1790−1794.
(75) Ahn, K.; Tsokol, A. O.; Mozharivskyj, Y.; Gschneidner, K. A.; Pecharsky, V. K. *Phys. Rev. B* **2005**, *72*, 054404−054415.
(76) He, J.; Ling, G.; Jiao, Z. *Physica B* **2001**, *301*, 196−202.
(77) Dremoa, R. V.; Koblyuk, N.; Mudryk, Y.; Romak, L.; Sechovsk, V. *J. Alloys Compd.* **2001**, *317−318*, 293−296.
(78) Katoh, K.; Tsutsumia, T.; Yamadaa, K.; Teruia, G.; Niidea, Y.; Ochiai, A. *Physica B* **2006**, *373*, 111−119.
(79) Varma, C. M. *Rev. Mod. Phys.* **1976**, *48*, 219−238.
(80) Peter, S. C.; Malliakas, C. D.; Nakotte, H.; Kothapilli, K.; Rayaprol, S.; Schultz, A. J.; Kanatzidis, M. G. *J. Solid State Chem.* **2012**, *187*, 200−207.